Calcium wave propagation in chains of endothelial cells with nonlinear reaction dynamics: Green's function approach

Pierre A. Deymier,[1] Keith Runge,[1] Martin J. Deymier,[2] James B. Hoying,[3] and Jérôme O. Vasseur[4]
[1]*Materials Science and Engineering Department, University of Arizona, Tucson, Arizona 85721, USA*
[2]*Department of Biochemistry and Department of Molecular Cell Biology, University of Arizona, Tucson, Arizona 85721, USA*
[3]*Cardiovascular Innovation Institute, Louisville, Kentucky 40292, USA*
[4]*IEMN, UMR CNRS 8520, Université de Lille 1, 59655 Villeneuve d'Ascq, France*
(Received 5 June 2010; revised manuscript received 22 August 2010; published 18 October 2010)

We present a Green's function-based perturbative approach to solving nonlinear reaction-diffusion problems in networks of endothelial cells. We focus on a single component (Ca^{2+}), piecewise nonlinear model of endoplasmic calcium dynamics and trans-membrane diffusion. The decoupling between nonlinear reaction dynamics and the linear diffusion enables the calculation of the diffusion part of the Green's function for network of cells with nontrivial topologies. We verify analytically and then numerically that our approach leads to the known transition from propagation of calcium front to failure of propagation when the diffusion rate is varied relative to the reaction rates. We then derive the Green's function for a semi-infinite chain of cells with various boundary conditions. We show that the calcium dynamics of cells in the vicinity of the end of the semi-infinite chain is strongly dependent on the boundary conditions. The behavior of the semi-infinite chain with absorbing boundary conditions, a simple model of a multicellular structure with an end in contact with the extracellular matrix, suggests behavioral differentiation between cells at the end and cells embedded within the chain.

DOI: 10.1103/PhysRevE.82.041913 PACS number(s): 87.18.Mp, 87.18.Fx, 87.18.Hf, 87.17.Pq

I. INTRODUCTION

From tumorigenesis, to tissue engineering to blood vessels, questions concerning the interactions between living cells and their environment/architecture have received increasing attention [1–9]. One aspect particularly relevant to these questions is the emerging behavior of a multicellular architecture in which cell-level functions, such as intracellular pathways, integrate with the architecture through cell-to-cell interactions. For example, downstream and upstream signal conduction between endothelial cells along the walls of vessels is playing an important role in circulatory function of formed vasculatures, vascular network remodeling, vasculogenesis and neovascularisation [10]. Central to this problem is that cellular networks inherently combine dynamical and structural complexity. Some mathematical approaches have tackled the problem by setting aside the dynamics of the network nodes (cells) and emphasizing the complexity of the network architecture [11]. On the other hand, Othmer and Scriven [12] developed, following Turing's pioneering mathematical treatise of morphogenesis [13], an approach in which the information about the underlying network topology, through a connectivity matrix, is decoupled from that of the intracellular reaction pathway dynamics thus incorporating complexity at the level of the cell and the network. In a series of studies [14,15], we used the Green's function-based interface response theory (IRT) [16], a method originally developed for studying composite media in condensed matter physics, to augment Scriven-Othmer's method to investigate coupled dynamical networks with nontrivial connectivity matrices and therefore study cell dynamics in complex network architectures. Using a linear model of the reaction dynamics of intracellular Ca^{2+} and inositol triphosphate (IP_3) negative feedback loop in endothelial cells, we showed the existence of propagating oscillatory compositional waves that were affected by the topology of the cell networks. Considering models of networks comprised of a main chain of endothelial cells and multiple side chains in ordered, defected, or disordered topologies, we observed that the transmission spectra of the compositional waves encode architectural information separately in terms of spatial arrangement and branch length via scattering and resonant filtering, respectively. From a biological point of view, to decode these signals, individual cells would need cellular control on frequency-dependent intracellular pathways such as protein phosphorylation by a Ca^{2+}-calmodulin activated kinase which is ubiquitous in a variety of cell types [17].

Plahte [18,19] argued that linear analysis of reaction-dynamics problems must be complemented by nonlinear analysis to effectively explain pattern formation. Of particular interest in the study of systems with nonlinear reaction dynamics is the phenomenon of propagation failure, where the wave speed is zero. In a model of a chain of nearest-neighbor, diffusively coupled, overdamped oscillators the propagation failure and the nature of the wave front depends on the nonlinearity of the dynamics of the model [20]. Similar behavior has been observed in a discrete version of Nagumo equation modeling excitable cells with a cubic dynamics [21]. There, propagation of a wave front occurs when the strength of the diffusion coupling is large enough. Similar results have been obtained by Kladko *et al.* [22]. Propagation failure of traveling waves in two-dimensional discrete lattice with nearest-neighbor diffusive-coupling and bistable scalar ODE at each site has demonstrated the angular dependency of the zero speed conditions through the detuning parameter of the nonlinearity [23].

In this context, the present paper focuses on the development of a Green's function-based approach for modeling

diffusion-reaction problems with nonlinear reaction dynamics. The goal is to implement a framework that would enable the use of IRT for studying the propagation of compositional waves in complex multicellular networks with nonlinear reaction dynamics. We set out to develop a theoretical model of information transmission along chains of endothelial cells based on wavelike Ca^{2+} signals, which are considered important, for instance, in vascular function [24]. In Sec. II of this paper, we present in details the development of a Green's function-based approach for solving the diffusion-reaction problem with intracellular Ca^{2+} nonlinear reaction dynamics and chains of endothelial cells. The decoupling between reaction dynamics and diffusion enables us to introduce a short-time propagator that can be used to predict the time evolution of calcium concentration. We show that the form of our propagator with linear dynamics is completely equivalent to that introduced by Othmer and Scriven [12]. We apply the Green's function approach in Sec. III to tackling the problem of propagation failure of a calcium wave front in an infinite chain of endothelial cells and we verify that the behaviors we observe are qualitatively comparable to those already reported in the literature [21,22]. Moreover, we show that our formalism is completely compatible with the IRT and we derive analytic expressions for the nonlinear reaction-diffusion propagator in semi-infinite chains of cells with various boundary conditions. We demonstrate theoretically for the first time that the dynamics of the calcium concentration in cells in the vicinity of the end of the semi-infinite chain is strongly dependent on the boundary conditions suggesting behavioral differentiation between cells in nonhomogeneous multicellular architectures. Finally conclusions are drawn in Sec. IV as to the applicability of our approach to more complex endothelial cell networks as well as to its biological relevance.

II. MODELS AND METHODS

A. Background

At the level of the individual cell, Ca^{2+} signals rely on the intake or release of Ca^{2+} ions from intracellular stores such as the endoplasmic reticulum (ER). The physiological state of the cytoplasm of a cell determines the nature of the dynamics of calcium release and intake [25]. Within endothelial cells of arterioles, a calcium based signaling pathway exists that contains a two-component negative feedback loop. This loop occurs between Ca^{2+} and IP_3. This inositol phospholipid signaling pathway is started by an extracellular signal molecule that activates a transmembrane G-protein coupled receptor which in turn activates phospholipase C-β. Phospholipase C-β cleaves intracellular membrane bound phospho inositol 4,5-bisphosphate $[PI(4,5)P_2]$ causing the cytoplasmic release of IP_3. Cytoplasmic IP_3 can bind and open IP_3 gated Ca^{2+} channels in the endoplasmic reticulum leading to increased cytoplasmic Ca^{2+} concentration. IP_3 concentration is degraded by phosphorylation via Ca^{2+} regulated kinase. The cytoplasmic inositol 1,4,5-triphosphate 3-kinases (IP_3Ks) are a group of calcium-regulated inositol polyphosphate kinases that convert IP_3 into inositol 1,3,4,5-tetrakisphosphate. This later specie is inactive as a Ca^{2+} release inducer, thus reducing intracellular Ca^{2+} concentration. The overall effect of this signaling cascade is that of a two component (Ca^{2+} and IP_3) negative feedback loop. Consequently, the physiological state of a cell may be bistable with two resting states for calcium concentration; low basal and high corresponding to replete ER and empty ER, respectively, and separated by an intermediate unstable threshold concentration. The bistable state may lead to traveling fronts in spatially extended systems. The physiological state may also be that of an excitable cytoplasm, and may be considered to be a variant on the bistable state with the possibility of returning to the low basal concentration beyond a high cytosol concentration threshold. Excitable cytoplasm may produce pulse waves in spatially extended systems. There exist a large variety of mathematical models of calcium dynamics and calcium waves [25–28]. However, since the objective of the present work is to demonstrate the feasibility of a Green-function-based approach to solving diffusion-reaction problems with nonlinear reaction dynamics, for the sake of mathematical tractability, we assume an effective nonlinear intracellular reaction dynamics involving only Ca^{2+}. For this we utilize a simple piecewise-linear model of the nonlinear Ca^{2+} reaction dynamics. This model mimics the Ca^{2+} depletion of the cytoplasm and repletion separated by a threshold concentration. Such piece-wise linear models have been shown to possess the essential features of nonlinear biological dynamical systems [29,30].

The development of the Green's function-based theory of complex multicellular architectures with nonlinear reaction dynamics is enabled by the convergence of three areas. The first area is the development of a theory of complex multicellular architectures with linear reaction dynamics that provides solutions that can be used as starting approximations for perturbative methods to be applied to architectures with nonlinear dynamics. This approach is based on the interface response theory (IRT) [16]. The second area relates to the so-called adiabatic switching formalism used in statistical mechanics for the calculation of the free energy of a system of interest by connecting it through a reversible path to a system with a known free energy. An effective Hamiltonian is constructed as a linear combination of the Hamiltonians of the two systems using a continuous variable [31,32]. In fact, this approach is similar to He's homotopy perturbation method (HPM) [33]. Here, an operator is separated into its linear and nonlinear parts. An embedding parameter that can vary between 0 and 1 is used to construct an operator that can transition between the linear operator and the nonlinear one. The solution to the switching operator is assumed to be expandable into a power series of the embedding parameters. Upon taking the limit of the embedding parameter toward 1 one obtains an approximate solution to the original nonlinear operator. The HPM has been shown to be able to effectively solve strongly nonlinear problems including nonlinear parabolic differential equations [34]. The final area is the use of Lippman-Schwinger equation or propagator theory for time dependent processes that enables us to write the Green's function of a perturbed system in terms of a series of integral terms involving the product of Green's function of the unperturbed system and of the perturbation operator. These perturbation expansions of the Green's function have been sum-

marized in the form of Feynman diagrams which have found applications in both high energy and condensed matter physics [35,36].

In the rest of this section, we address the treatment of linear and nonlinear reaction dynamics with Green's function approaches. We then turn to extending this approach to include spatial degrees of freedom in the case of the linear reaction- and nonlinear reaction-diffusion problems.

B. Linear and nonlinear reaction dynamics

We address the problem of linear and nonlinear reaction dynamics to establish the mathematical foundations in terms of Green's functions that will enable us to derive an expression for a time propagator. Let us first start with a simple linear reaction problem where the kinetics of the reaction is described by the following equation:

$$\frac{du}{dt} = -Ku \tag{1}$$

where K is the reaction rate (taking positive or negative values), and u some composition variable. The solution to that equation is obtained by integration over time and takes the form

$$u(t) = u(t')e^{-K(t-t')}. \tag{2}$$

Equation (1) can also be solved by using Laplace transforms. It becomes

$$\omega\tilde{u} - u(0) = -K\tilde{u}, \tag{3}$$

ω is the variable conjugated with time in the transform.

The Laplace transform of the composition is obtained as

$$\tilde{u} = u(0)\frac{1}{\omega + K}. \tag{4}$$

The inverse Laplace transform of Eq. (4) gives the solution of Eq. (2) where t' is taken as the origin of time.

Finally, one may recast Eq. (1) in terms of a time dependent Green's function or propagator, $G(t-t')$, in the form

$$LG(t-t') = \delta(t-t'), \tag{5}$$

where the operator L is defined as

$$L = \frac{d}{dt} + K. \tag{6}$$

The solution to Eq. (5) is given by

$$G(t-t') = H(t-t')e^{-K(t-t')}. \tag{7}$$

In Eq. (7), $H(t-t')$ is the Heaviside function with

$$H(t-t') = \begin{cases} 0 & \text{if } t \le t' \\ 1 & \text{if } t > t' \end{cases}. \tag{8}$$

The solution for the composition is recovered by the time integration of the product of the propagator and some initial condition $u(0)$. For instance using, $t=0$ as origin of time and $u(0)=u_0\delta(t)$ with δ being the usual delta function, the time dependence of the composition is obtained as

$$u(t) = \int_{-\infty}^{\infty} H(t-t')e^{-K(t-t')}u_0\delta(t')dt' = u_0e^{-Kt}.$$

Let us now consider a single component nonlinear reaction problem that can be modeled via a two-segment piecewise linear function. The differential equation which solution is the time evolution of the composition, $u(t)$, is written as

$$\frac{\partial u}{\partial t} + [1 - H(u-u_c)]K_1u + H(u-u_c)K_2u = 0 \tag{9}$$

Here K_1 and K_2 are the reaction rates of the linear segments. u_c is the composition at which the system can switch between state 1 (reaction rate K_1) and state 2 (rate K_2). H is the Heaviside function or any other function that might describe the transition from one reaction rate to another upon change in composition.

He's homotopy perturbation method (HPM) starts with the differential equation

$$A(u) = 0, \tag{10}$$

where A is a general differential operator than can be divided into a linear part, L and a nonlinear part N. The differential equation then becomes

$$L(u) + N(u) = 0. \tag{11}$$

If the solution of the linear differential equation $L(u)=0$ is u_L, then one rewrites the general differential equation in the form,

$$L(u) + (1-p)L(u_L) + pN(u) = 0 \tag{12}$$

where p is an embedding parameter. The parameter p varies between 0 and 1 and continuously links the linear problem to the nonlinear one of interest. When $p=0$, the problem reduces to the linear one with solution u_L. In the case $p=1$, the differential equation becomes the original one. Assuming that the solution of Eq. (10) can be written in the form of a power series in p, in the limit of $p \to 1$, one recovers the solution to the nonlinear problem of interest. We illustrate the extension of He's HPM with propagator's theory to solve a nonlinear reaction differential equation. Replacing H in Eq. (9) by an embedding parameter p, Eq. (9) becomes isomorphic to Eq. (12). When $p=0$, and $p=1$, Eq. (9) becomes a set of two linear equations extending over the complete interval of values accessible to u,

$$\frac{\partial u}{\partial t} + K_1u = 0,$$

$$\frac{\partial u}{\partial t} + K_2u = 0. \tag{13}$$

Introducing the Green's function formalism, Eqs. (13) take the form,

$$\left(\frac{\partial}{\partial t} + K_i\right)G_i^0(t-t') = \delta(t-t') \text{ with } i = 1,2, \tag{14}$$

with solutions

$$G_1^0(t-t') = H(t-t')e^{-K_1(t-t')},$$

$$G_2^0(t-t') = H(t-t')e^{-K_2(t-t')}. \quad (15)$$

Equation (9) also becomes

$$\left[\frac{\partial}{\partial t} + K_1 + p(K_2 - K_1)\right] G(t-t') = \delta(t-t'), \quad (16)$$

where the third term in the parenthesis can be thought of as a perturbation operator

$$V = p(K_1 - K_2). \quad (17)$$

To progress further, let us make for now the assumption that the perturbation V is independent of time, i.e., we make the Eikonal approximation for slow varying perturbations to calculate time integrals. We may take the value of the embedding parameter to be that corresponding to the initial composition, $p[u(0)]$.

Considering a system described by a Green's function, G_1^0, the Green's function, G, for this same system but perturbed by the operator, V, satisfies the Lippmann-Schwinger equation,

$$G(t-t') = G_1^0(t-t') - \int_{-\infty}^{+\infty} dt'' G_1^0(t-t'')VG_1^0(t''-t') + \int_{-\infty}^{+\infty} dt'' \int_{-\infty}^{+\infty} dt''' G_1^0(t-t'')VG_1^0(t''-t''')VG_1^0(t'''-t') - \cdots. \quad (18)$$

Inserting Eq. (15) into Eq. (18) and performing the appropriate integrations for times before or after switching, one obtains

$$G(t-t') = H(t-t')e^{-K_1(t-t')}\left[1 - V(t-t') + \frac{1}{2}V^2(t-t')^2 - \frac{1}{6}V^3(t-t')^3 \ldots\right]. \quad (19)$$

Equation (19) is a power series in V and therefore p. One notes that when $p=0$ $[H(u-u_c)=0$ or $u<u_c]$ the solution to the problem is that of the differential equation with linear dynamics and rate constant K_1. The embedding parameter allows the transition from the state 1 to the state 2 (solution of the differential equation with reaction constant K_2). The parenthesis in Eq. (19) converges to $e^{-V(t-t')}=e^{-p(K_2-K_1)(t-t')}$ and in the limit $p=1$ $[H(u\text{-}u_c)=1$ or $u>u_c]$, G converges to G_2^0.

The solution for the propagator in the case of a constant perturbation (p) takes the form

$$G(t-t') = H(t-t')e^{-K_1(t-t')}e^{-p(K_2-K_1)(t-t')}. \quad (20)$$

Again, in performing the integrals in Eq. (18), we have considered that the perturbation operator V and therefore the embedding parameter p are independent of time. However, it is clear in Eq. (9) that the embedding parameter represents a transition function of composition which is time dependent. Consequently, the Green's function or propagator of the perturbed system given by Eq. (20) cannot be used as is to represent the solution of the nonlinear dynamics problem with time dependent embedding parameter. We therefore use an iterative process to solve the nonlinear dynamics of the system. Let us consider a small time difference, $\delta t=t-t'$, with known composition at t', $u(t')$, we assume that $p(u(t))$ takes the constant value $p(u(t'))$ during that interval of time. This enables us to propagate the composition using Eq. (20) to the later time t. At that time, the new composition is used to determine the new value of the embedding parameter and propagates the composition further in time. Equation (20) can therefore be used iteratively as a propagator over only small time intervals δt. The size of the time interval depends on the nature of the function describing the composition dependence of the embedding parameter.

The solution of Eq. (9) can be also obtained by performing a Laplace transform assuming that p is independent of time over some time interval $[0,t]$ taking the value $p(u(0))$,

$$[\omega + k_1 + p(K_2 - K_1)]\tilde{u} = u(0). \quad (21)$$

The Laplace transform of the composition is

$$\tilde{u} = u(0)\frac{1}{\omega + K_1 + p(K_2 - K_1)}, \quad (22)$$

which leads to the sought solution when doing the inverse Laplace transform

$$u(t) = u(0)e^{-K_1 t}e^{-p(K_2-K_1)t}. \quad (23)$$

This solution is obtained by assuming that p is constant. Again, to account for the actual nonlinear reaction dynamics where the embedding parameter is composition (and time) dependent, one may use Eq. (23) in an iterative process over short-time intervals to solve for the time dependence of the composition over a series of short-time intervals starting from some known initial condition. The approach developed here will now be used to derive an analytical expression for the propagator of the reaction-diffusion problem of a chain of cells with nonlinear reaction dynamics.

C. Diffusion-reaction problem with linear or nonlinear reaction dynamics

The objective of this section is to add spatial degrees of freedom to the approach described in Sec. II A and derive an expression for the reaction-diffusion propagator with nonlin-

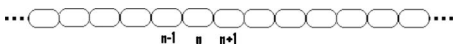

FIG. 1. Model of chain of cells.

ear reaction dynamics. We first tackle the problem of linear reaction kinetics in conjunction with diffusion. We consider a one-dimensional chain of cells as illustrated in Fig. 1.

The linear reaction-diffusion problem is described by the equation,

$$\frac{du_n}{dt} = W(u_{n+1} - 2u_n + u_{n-1}) - Ku_n. \tag{24}$$

The first term in the right-hand side of the equation represents the diffusion process between adjacent cells via the discrete Laplacian operator. From a biological point of view transmembrane diffusion may take place via gap junctions. The second term represents the linear reaction dynamics of cell "n." W relates to the nearest-neighbor calcium transfer rate. K is the reaction rate.

We can Laplace transform Eq. (24) which becomes

$$\omega\tilde{u}_n - u_n(0) = W(\tilde{u}_{n+1} - 2\tilde{u}_n + \tilde{u}_{n-1}) - K\tilde{u}_n. \tag{25}$$

In Eq. (25), $u_n(0)$ is the initial concentration profile along the chain. If we choose $u_n(0)=\delta_{nm}$ where δ_{nm} is the usual Kroenecker symbol as initial condition, that is a unit initial concentration at the cell "m," then Eq. (25) may be rewritten into the form

$$W\tilde{u}_{n+1} - (2W + \omega + K)\tilde{u}_n + W\tilde{u}_{n-1} = -\delta_{nm}. \tag{26}$$

The composition $\tilde{u}_n$ in Eq. (26) can therefore be thought as a spatial Green's function, $\tilde{D}_{n,m}$, that is the response of the system at location "n" to a delta stimulus at location "m." Eq. (26) can be rewritten in matrix form

$$W\begin{pmatrix} \cdots & 0 & 1 & -2\xi & 1 & 0 & 0 & \cdots \\ \cdots & 0 & 0 & 1 & -2\xi & 1 & 0 & \cdots \\ \cdots & 0 & 0 & 0 & 1 & -2\xi & 1 & 0 \end{pmatrix} \begin{pmatrix} \cdot \\ \tilde{D}_{n-1,m} \\ \tilde{D}_{n,m} \\ \tilde{D}_{n+1,m} \\ \cdot \end{pmatrix} = -\overleftrightarrow{I}. \tag{27}$$

In Eq. (27), $\overleftrightarrow{I}$, is the identity matrix and $\xi=1+\frac{(\omega+K)}{2W}$. The diffusion-reaction matrix on the left hand side of Eq. (27) is tridiagonal. The solution to Eq. (27) is known [37] and is given by

$$\tilde{D}_{n,m} = \frac{-1}{W}\frac{\tau^{|n-m|+1}}{\tau^2 - 1}, \tag{28}$$

with

$$\tau = \begin{cases} \xi - (\xi^2 - 1)^{1/2} & \text{if } \xi > 1 \\ \xi + (\xi^2 - 1)^{1/2} & \text{if } \xi < -1 \\ \xi + i(1 - \xi^2)^{1/2} & \text{if } -1 < \xi < 1 \end{cases}. \tag{29}$$

When K is positive, it is obvious that $\xi=1+\frac{(\omega+K)}{2W}>1$ and τ is given by the first relation in Eq. (29). When $K<0$, then we consider the inversion formula for the Laplace transform of some function, $F(\omega)$,

$$h(t) = \frac{1}{2\pi i}\int_{C-i\infty}^{C+i\infty} e^{\omega t}F(\omega)d\omega \tag{30}$$

In Eq. (30), the integration is along the imaginary axis with the real part of ω, C, taking any large positive value, thus enabling ξ to remain greater than 1 independently of the sign of K. We can also obtain the solution by considering $K=0$, then Eq. (28) can we rewritten as

$$\tilde{D}_{nm} = \frac{1}{\sqrt{\omega(\omega+4W)}}\left[\frac{2W}{(2W+\omega)+\sqrt{\omega(\omega+4W)}}\right]^{|n-m|}. \tag{31}$$

The inverse Laplace transform of Eq. (31) is given by [42]

$$D_{nm}(t) = e^{-2Wt}I_{|n-m|}(2Wt), \tag{32}$$

with $I_{|n-m|}$ being the modified Bessel function. Equation (32) is the Green's function for the diffusion problem along a discrete chain. If we now consider a nonzero reaction rate, K, we can make the change of variable $\omega'=\omega+K$ in Eq. (31). Here we used the fact that the sign of K does not impact the choice of the solution in Eq. (29) as discussed previously due to the nature of the inverse Laplace transform. We now use the relation $LT[e^{-at}h(t)]=F(\omega+a)$ with LT representing the Laplace transformation for all a's, positive or negative, to obtain

$$D_{nm}(t) = e^{-Kt}e^{-2Wt}I_{|n-m|}(2Wt). \tag{33}$$

Let us now treat the case of nonlinear reaction dynamics,

$$\frac{du_n}{dt} = W(u_{n+1} - 2u_n + u_{n-1}) - [K_1 + p(K_2 - K_1)]u_n \tag{34}$$

Following Sec. II A, we can now address this problem in the limit of short times, i.e., time intervals during which we assume that the embedding parameter, p, is constant. We are now in a position to write the sought expression for the reaction-diffusion propagator with nonlinear reaction dynamics. The Green's function propagator in the short-time interval is obtained in the form,

$$D_{nm}(t-t') = e^{-[K_1+p(K_2-K_1)](t-t')}e^{-2W(t-t')}I_{|n-m|}[2W(t-t')]. \tag{35}$$

Knowing an initial condition, the time evolution of the composition field in the one-dimensional chain of cells can therefore be obtained in an iterative manner according to

$$u_n(t+\delta t) = \sum_m D_{nm}(\delta t)u_n(t), \tag{36}$$

where δt is small.

D. Relation to Othmer's approach

Here, we will place Eq. (35) in the context of the approach of Othmer and Scriven. Othmer and Scriven, while

analyzing the onset of instability at homogeneous steady states of multicellular networks, developed an elegant method that decouples the intracellular biochemical dynamics from the network structure of an underlying reaction/diffusion problem [12]. They assumed a mixture of n reactants in each one of the N cells, each attached to one or more other cells to form the desired topology. The small excursions around the steady-state concentration values of cell μ is represented by the $n\times 1$ vector $\mathbf{u}^{(\mu)}$ which is solution of a linear vector differential equation given by

$$\frac{d\mathbf{u}^{(\mu)}}{dt} = \mathbf{W}\Delta^{(\mu)}\mathbf{u}^{(\mu)} + \mathbf{K}\mathbf{u}^{(\mu)}, \quad \mu = 1, \ldots, N. \tag{37}$$

Equation (37) is the extension of Eq. (24) to multiple reactants. The elements, W_{ij}, $i,j=1,\ldots,n$, of the $n\times n$ transfer matrix $\boldsymbol{W}$ quantify the effect of reactant j on the transfer of reactant i through the barrier separating adjacent cells. The Laplacian $\Delta^{(\mu)}\mathbf{u}^{(\mu)}=\mathbf{u}^{(\mu+1)}(t)-2\mathbf{u}^{(\mu)}(t)+\mathbf{u}^{(\mu-1)}(t)$ encodes the connection pattern among the cells as also described in Eq. (24). The Laplacian of a chain of N cells is a $N\times N$ matrix. We use $\mathbf{C_x}$ to represent the resulting structural matrix. For instance the structural matrix $\mathbf{C}_\infty$ of an infinite chain of cells (see Fig. 1) has the familiar tridiagonal form [see Eq. (27)]

$$\mathbf{C}_\infty = \begin{pmatrix} \ddots & \ddots & \ddots & \ddots & & & & & \\ \ddots & \ddots & \ddots & \ddots & \ddots & & & & \\ \cdots & 0 & 1 & -2 & 1 & 0 & \cdots & & \\ & \cdots & 0 & 1 & -2 & 1 & 0 & \cdots & \\ & & \cdots & 0 & 1 & -2 & 1 & 0 & \cdots \\ & & & \cdots & 0 & 1 & -2 & 1 & 0 & \cdots \\ & & & & & \ddots & \ddots & \ddots & \ddots & \ddots \\ & & & & & & \ddots & \ddots & \ddots & \ddots \end{pmatrix}. \tag{38}$$

The three nonzero entries in each row correspond to the coefficients in the discrete approximation of the Laplacian.

The reaction matrix $\mathbf{K}$ represents a linearized intracellular reaction dynamics with the elements, k_{ij}, $i,j=1,\ldots,n$, representing the collective effect of reactant j on the reactant i. The time evolution of concentration excursions in all of the cells is concatenated into a $Nn\times 1$ column vector given by

$$\mathbf{u}(t) = \sum_{k=1}^{N} \mathbf{x}_k \otimes e^{(\mathbf{K}+\alpha_k\mathbf{W})t}\mathbf{y}_k^0, \tag{39}$$

with $\otimes$ representing the tensor product. In Eq. (39), α_k and $\mathbf{x}_k$, $k=1,\ldots,N$, are the Eigen values and Eigen vectors of the connectivity matrix, $\mathbf{C_x}$, respectively. The $n\times 1$ vector $\mathbf{y}_k^0$ is the projection of the initial condition vector $\bar{\mathbf{u}}_0=\mathbf{u}(t=0)$ onto a derived set of basis vectors spanning the vector space that includes $\mathbf{u}(t)$, η_j, $j=1,2,\ldots,n$ with $\eta_j=[0,0,\ldots,0,1^{j^{th}position},0,\ldots,0]^T$.

$\mathbf{y}_k^0$ is therefore given by

$$\mathbf{y}_k^0 = \sum_{j=1}^{N} \langle \mathbf{u}_0, \mathbf{x}_k \otimes \eta_j \rangle \eta_j. \tag{40}$$

The terms between brackets in Eq. (40) take the form,

$$\langle \mathbf{u}_0, \mathbf{x}_k \otimes \eta_j \rangle = \sum_{m=-\infty}^{+\infty} \mathbf{u}_0^{(j+mn)} . \mathbf{x}_k^{*m}. \tag{41}$$

In Eq. (41), the * stands for the complex conjugate. To illustrate the construction of a solution for the composition along an infinite chain, we write the Eigen values and Eigen vectors corresponding to the operator matrix of Eq. (38) [38],

$$\alpha_k = -4\sin^2\left(\frac{ka_0}{2}\right),$$

$$\mathbf{x}_k = (\ldots \quad e^{-ika_0} \quad 1 \quad e^{ika_0} \quad \ldots)^T, \tag{42}$$

where k is the propagation constant and a_0 is the lattice constant spacing between cells. Note that for the infinite chain, k is a continuous variable and that the discrete summation in Eq. (39) has to be replaced by an integral, that is $\sum_{k=-\infty}^{\infty} \to \int_{-\pi}^{\pi} \frac{dk}{2\pi}$. $\mathbf{x}_k$ is a discrete complex sinusoidal function with wave number k. k is a measure of the spatial variation of the Eigenvectors. The Eigenvectors of Eq. (42) correspond to propagating waves, taking $a_0=1$ as unit of length, these are periodic functions in $k'=ka_0$ defined over the interval $[-\pi,\pi]$. Notice that each Eigenvector is of infinite length and its mth element $u_{k,m}$ represents the mth cell in the chain, where m is an integer.

We now apply the approach to a single component $n=1$ problem. We use an initial condition, $u_0^{(\mu)}=\delta_{\mu m}$, that is a delta concentration at cell m. With this initial condition, $u^{(\mu)}=D_{\mu m}$ that is the spatial Green's function of the Diffusion-reaction problem. In this case Eq. (39) takes the simple form

$$u^{(\mu)} = \int \frac{dk}{2\pi} e^{(K+\alpha_k W)t} e^{ika_0(\mu-m)}. \tag{43}$$

In Eq. (43), K and W are scalar quantities for a single component reaction.

Inserting the Eigenvalues and Eigenvectors of the infinite chain into Eq. (43) gives:

$$u^{(\mu)} = e^{Kt} \int \frac{dk}{2\pi} e^{\left(-4\sin^2\frac{ka_0}{2}W\right)t} e^{ika_0(\mu-m)} \tag{44}$$

We then use the trigonometric identity $\sin^2\theta=\frac{1}{2}-\frac{1}{2}\cos 2\theta$ to cast Eq. (44) in the form

$$u^{(\mu)} = e^{Kt}e^{-2Wt} \int \frac{dk}{2\pi} e^{2Wt\cos(ka_0)} e^{ika_0(\mu-m)}. \tag{45}$$

We need to consider only the real part of the integral in Eq. (45),

$$\mathrm{Re}\left(\int dk e^{2Wt\cos(ka_0)} e^{ika_0(\mu-m)}\right) = \int dk e^{2Wt\cos(ka_0)}\cos[ka_0(\mu-m)]. \quad (46)$$

Taking $a_0=1$, and in light of the evenness of the cosine function, we replace $\mu-m$ by its absolute value $|\mu-m|$ and the integral in Eq. (46) reduces to the modified Bessel function,

$$I_{|\mu-m|}(2Wt) = \frac{1}{\pi}\int_0^{\pi} dk e^{2Wt\cos k}\cos(k|\mu-m|). \quad (47)$$

With Eq. (47), we recover the solution of Eq. (33) for the case of linear reaction dynamics.

Again, the separation of the reaction dynamics and the diffusion dynamics in Eq. (39), suggests that we can use this very same solution to develop a short-time propagator for a nonlinear reaction dynamics using an embedding parameter, i.e., to obtain Eq. (35). It is therefore possible to use Othmer's approach to solving the diffusion-reaction problem with linear reaction dynamics to develop expressions for the propagator of the nonlinear dynamics over short-time intervals. The application of the method presented here to more complex multicellular networks relies on the knowledge of the connectivity matrix and their corresponding Eigenvectors and Eigenvalues.

III. RESULTS

A. Propagation failure in a one-dimensional chain of cells

Let us treat the problem of a chain of cells with variable calcium concentration due to intake and release by endoplasmic reticulae (ER). This case can be treated by considering the nonlinear reaction dynamics with $K_1>0$ and $K_2<0$. From the point of view of an isolated cell, when the calcium concentration is less than the critical value u_c, the ER deplete the endoplasm. When the calcium concentration exceeds the critical value, the ER releases calcium into the cell.

We consider solutions to the nonlinear reaction dynamics-diffusion problem in the form of propagating waves, that is

$$u_n(t) = \varphi(n-ct). \quad (48)$$

In Eq. (48), position is expressed in units of $a_0=1$ by the integer n. c is the wave velocity.

Inserting this general form into Eq. (36) gives

$$\varphi[n-c(t+\delta t)] = e^{-[K_1+p(K_2-K_1)]\delta t}e^{-2W\delta t}\sum_m I_{|n-m|}(2W\delta t)\varphi(m-ct). \quad (49)$$

It is convenient to define: $\zeta_n=n-ct$ and take $\delta t=1/c$ as the time for a one step motion. With these definitions, Eq. (49) reduces to

$$\varphi(\zeta_{n-1}) = e^{-[K_1+p(K_2-K_1)]\delta t}e^{-2W\delta t}\sum_m I_{|n-m|}(2W\delta t)\varphi(\zeta_m). \quad (50)$$

We assume that the function φ is single valued. In that case, $p=H[\varphi(\zeta_n-u_c)]=h(\zeta_n)$. We can choose without loss of generality, the point ζ_n where the composition is equal to the critical value for switching between rate K_1 and rate K_2,

$$\varphi(\zeta_n) < u_c \text{ for } \zeta_n < 0, \qquad \varphi(\zeta_n) > u_c \text{ for } \zeta_n > 0. \quad (51)$$

If follows that we can also write

$$e^{-[K_1+p(K_2-K_1)]\delta t} = e^{-K_1\delta t} + h(\zeta_n)[e^{K_2\delta t} - e^{-K_1\delta t}]. \quad (52)$$

Inserting all this into Eq. (5) gives

$$\varphi(\zeta_{n-1}) = [e^{K_1/c} + h(\zeta_n)[e^{K_2c} - e^{K_1/c}]]e^{-2W/c}\sum_m I_{|n-m|} \times (2W/c)\varphi(\zeta_m). \quad (53)$$

Equation (53) provides a means of calculating the velocity of the wave, c, in terms of the diffusion constant W and of the reaction rates, K_1 and K_2.

We assume that $u_c=0.5$ and we now make a simple piecewise linear approximation to the wave solution, φ,

$$\varphi(\zeta_n) = \begin{cases} 1 \text{ if } \zeta_n > 2b \\ 0 \text{ if } \zeta_n < -2b \\ \frac{1}{2} + \frac{\zeta_n}{4b} \text{ if } -2b < \zeta_n < 2b \end{cases}. \quad (54)$$

The parameter b represents the width of the transition region between the two calcium concentrations 0 and 1. This function represents the propagation of a concentration front. With this solution, the summation in Eq. (53) becomes

$$\sum_m I_{|n-m|}(2W/c)\varphi(\zeta_m) = \sum_{-2b}^{2b} I_{|n-m|}(2W/c)\left(\frac{1}{2}+\frac{\zeta_m}{4b}\right) + \sum_{m>2b} I_{|n-m|}(2W/c). \quad (55)$$

We rewrite Eq. (53) at two points along the concentration profile, namely, $n=1$ and $n=-1$. We obtain a set of two equations

$$\frac{1}{2} = e^{-K_2/c}e^{-2W/c}\left[\sum_{-2b}^{2b} I_{|1-m|}(2W/c)\left(\frac{1}{2}+\frac{\zeta_m}{4b}\right) + \sum_{m>2b} I_{|1-m|}(2W/c)\right] \text{if } n=1,$$

$$\frac{1}{2}-\frac{1}{2b} = e^{-K_1/c}e^{-2W/c}\left[\sum_{-2b}^{2b} I_{|-1-m|}(2W/c)\left(\frac{1}{2}+\frac{\zeta_m}{4b}\right) + \sum_{m>2b} I_{|-1-m|}(2W/c)\right] \text{if } n=-1. \quad (56)$$

After extensive algebraic manipulations, using the properties of the modified Bessel functions, the set of Eqs. (56) can be simplified,

$$e^{\alpha}[e^{K_2/c}-1] = I_{2b}(\alpha) + I_{2b+1}(\alpha) + \frac{1}{b\alpha}\sum_{p=1}^{2b} p^2 I_p(\alpha) \quad \text{if } n=1,$$

$$\left(1-\frac{1}{b}\right)e^{\alpha}e^{K_1/c} = e^{\alpha} - [I_0(\alpha)+I_1(\alpha)+I_{2b}(\alpha)+I_{2b+1}(\alpha)] - \frac{1}{b\alpha}\sum_{p=1}^{2b} p^2 I_p(\alpha) \quad \text{if } n=-1, \quad (57)$$

where $\alpha=2W/c$.

We can obtain a relationship between the wave velocity, width and the physical parameters of the problem, namely diffusion coefficient and reaction rates by taking the sum of both Eqs. (57). This gives

$$e^{\alpha}\left[2-e^{K_2/c}-e^{K_1/c}\left(1-\frac{1}{b}\right)\right] = I_0(\alpha)+I_1(\alpha). \quad (58)$$

To determine the wave velocity, it is easier to define $x=1/c$ and recast Eq. (58) in the form

$$f(x,b) = 2-e^{K_2 x}-e^{K_1 x}\left(1-\frac{1}{b}\right) = e^{-2Wx}[I_0(2Wx)+I_1(2Wx)]$$
$$= g(x,W). \quad (59)$$

Using Eq. (59), we can study the condition for propagation of the compositional front wave as a function of the front width, diffusion and reaction parameters. For the sake of illustration, we plot in Fig. 2, the functions $f(x,b)$ and $g(x,W)$ representing the left-hand side and right-hand side of Eq. (59) for a variety of widths of the wave front, b, and diffusion constant W, as functions of x. For simplicity we also take the rate of calcium release and intake of the calcium stores to be equal in magnitude, i.e., $K_1=1$ and $K_2=-1$.

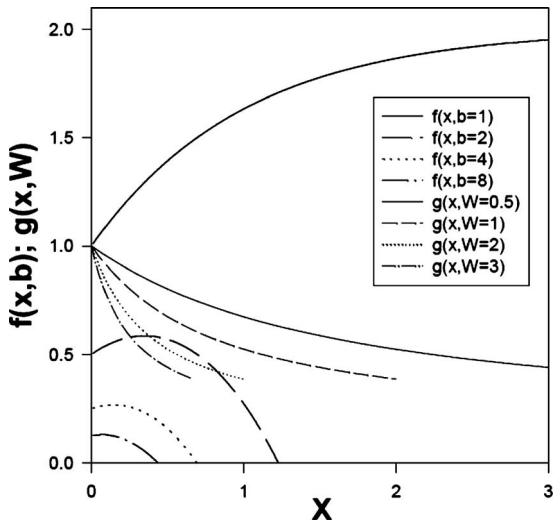

FIG. 2. Functions $f(x,b)$ and $g(x,W)$ for case $K_1=1$ and $K_2=-1$ and $u_c=0.5$.

The intersection points between the functions $f(x,b)$ and $g(x,W)$ correspond to the solutions of Eq. (59). There is propagation failure of the compositional wave when the two curves do not intersect. For instance, a front with $b=2$ does not propagate unless the diffusion constant exceeds a value somewhere between 1 and 2. A physically unrealistic very narrow wave front ($b=1$) appears to have a single solution for $x=0$ independently of the diffusion coefficient. This solution corresponds to an infinite wave velocity, c. There appears to exist two solutions for the speed for fronts with $b>1$ and diffusion coefficients $W>2$. It is important to note that the particular details of the functions f and g as well as the solutions of Eq. (59) may be artifacts due to the choice of a spatially symmetric piecewise linear function as an approximate solution of the concentration wave front. The main point that needs to be retained from this approximate analysis is that conditions in terms of diffusion and reaction dynamics may exist for which a wave front may experience propagation failure.

To investigate the failure of propagation further, we develop two numerical algorithms. The first one is a simple finite difference time domain (FDTD) method applied to solving the nonlinear reaction-diffusion equation. All rates, W, K_1, and K_2 have dimension of inverse time. Since $W\delta t$ is a dimensionless quantity, transfer rates, reaction rates and time interval will be expressed as dimensionless quantities in the rest of the paper. The second approach makes use of the propagator in Eqs. (35) and (36). The second approach uses a short-time approximation to the modified Bessel function [39], namely,

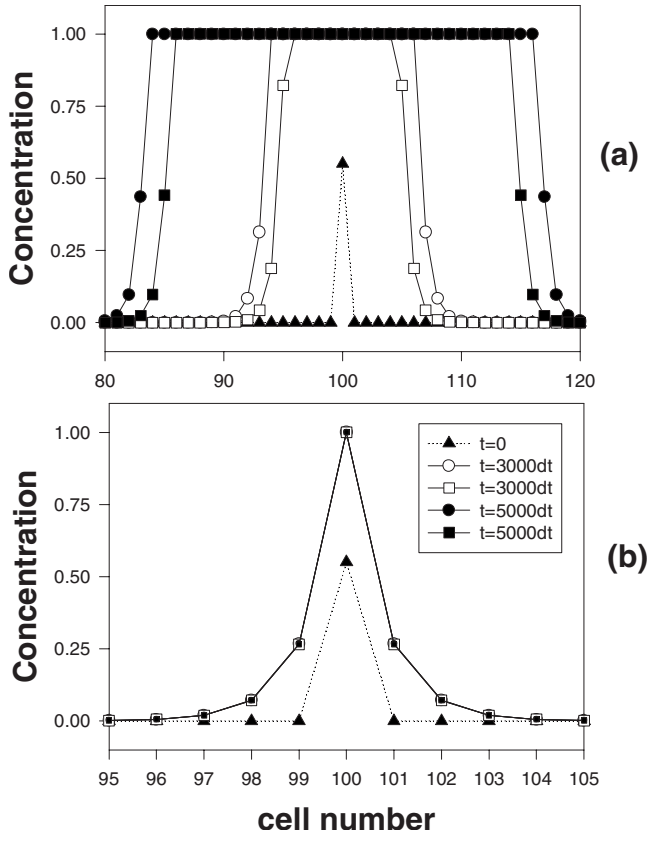

FIG. 3. Time evolution of calcium concentration profile for (a) $W=0.7$, $K_1=1$, $K_2=-1$ and (b) $W=0.5$, $K_1=1$, $K_2=-1$. The open symbols correspond to finite difference time domain solutions. The closed symbols correspond to solutions obtained with Green's function-based algorithm. The close triangles are the initial condition. $\delta t=0.01$ and $u_c=0.3$.

$$I_{|n-m|}(2W\delta t) \cong \frac{(W\delta t)^{|n-m|}}{|n-m|!}. \tag{60}$$

The nonlinear reaction dynamics is supplemented with a cap at a concentration of 1. The FDTD algorithm is significantly faster computationally than its Green's function counterpart since the evaluation of the discrete Laplacian involves only nearest-neighbor cells. The Green's function algorithm, however, requires the computationally expensive summation of Eq. (36). We have found a computational compromise between accuracy and computing time by choosing a time step of $\delta t=0.01$. The convergence of the algorithm depends on the number of cell with nonzero contributions to the summation in Eq. (36). As the number of such contributions increases, convergence requires a decrease in the time step. Figure 3 illustrates the transition from propagation to propagation failure of the concentration wave. The conditions of the calculations are given in the caption. These conditions differ from those of Fig. 2 as the later were obtained for an approximate analytical solution. More specifically, we use the critical concentration, $u_c=0.3$ to observe propagation and propagation failure with $K_1=-K_2=1$ and $W<1$. The initial condition is a delta concentration located at cell 100 and exceeding the concentration threshold of the nonlinear reaction dynamics. Figure 3(a) shows the propagation of two symmetrical fronts from that initial condition. The deviations between the concentration profiles obtained with the FDTD and Green's function methods are the result of accumulation of errors due to the approximation made in Eq. (60). It is therefore clear that when $W=0.7$, $K_1=1$, and $K_2=-1$, wave propagation takes place. The width of the wave front includes approximately 4 to 5 cells and is not described correctly by a linear function. Reducing the diffusion constant, W, from 0.7 to 0.5 leads to a transition to a nonpropagating mode. Propagation failure leads to a concentration profile that does not evolve with time. Using the FDTD approach, the transition between front propagation and propagation failure occurs for a diffusion constant $W=0.6109$. We note that the two algorithms agree very well numerically since the number of cells contributing to the summation in Eq. (36) is small. The concentration profile at steady state has a half-width of approximately 4 to 5 cells consistent with that of the propagating front.

In summary, from the numerical calculations, it is clear that the analytically derived Eq. (59) and corresponding Fig. 2 can only be used in a qualitative fashion due to the piecewise symmetrical approximation made in defining the shape of the concentration front. However, this approach shows qualitatively that a transition from propagation to propagation failure occurs as the diffusion constant decreases. From a numerical point of view, the Green's function approach is computationally more expensive than the FDTD method. The Green's function approach will give an advantage when considering finite chains of cells with cells at their ends obeying absorbing boundary conditions as such conditions are not trivial to implement in a FDTD scheme. This topic is addressed in the next section.

Finally, both analytical and numerical approaches show propagation failure of a calcium wave front in an infinite chain of endothelial cells. This behavior is qualitatively comparable to other examples of propagation failure of front already reported in the literature [21,22]. More specifically, our models show the known behavior of a transition from propagation to propagation failure when the diffusion rate is varied relative to the reaction rates.

B. Semi-infinite chain of cells with various boundary conditions

In this section, we illustrate the usefulness of the Green's function formalism to shed light on the effect of nonlinear dynamics on calcium wave behavior in chains of endothelial cells with ends. In particular we investigate the behavior of cells in the vicinity of the end of a semi-infinite chain. The formalism introduced in this paper decouples the diffusion problem from the reaction dynamics. We can therefore use the IRT [16] to determine the Green's function for diffusion along chains of cells with perturbations such as a free end. We consider the cleavage of an infinite chain of cells illustrated in Fig. 4 by severing the gap junctions between cells 0 and 1, that is, inhibiting diffusion between these two cells.

Let us consider a linear reaction with constant K. In this case Eq. (27) must be rewritten in the form

$$W\begin{pmatrix} . & 1 & 0 & 0 & 0 & 0 & 0 & 0 & 0 & . \\ . & -2\xi & 1 & 0 & 0 & 0 & 0 & 0 & 0 & . \\ . & 1 & -2\xi & 1 & 0 & 0 & 0 & 0 & 0 & . \\ . & 0 & 1 & -2\xi & 1 & 0 & 0 & 0 & 0 & . \\ . & 0 & 0 & 1 & -2\alpha & 0 & 0 & 0 & 0 & . \\ . & 0 & 0 & 0 & 0 & -2\alpha & 1 & 0 & 0 & . \\ . & 0 & 0 & 0 & 0 & 1 & -2\xi & 1 & 0 & . \\ . & 0 & 0 & 0 & 0 & 0 & 1 & -2\xi & 1 & . \\ . & 0 & 0 & 0 & 0 & 0 & 0 & 1 & -2\xi & . \\ . & 0 & 0 & 0 & 0 & 0 & 0 & 0 & 1 & . \end{pmatrix}\begin{pmatrix} . \\ \tilde{d}_{-1,m} \\ \tilde{d}_{0,m} \\ \tilde{d}_{1,m} \\ . \end{pmatrix} = -\overleftrightarrow{I}, \tag{61}$$

where $\xi = 1 + \frac{(\omega+K)}{2W}$ and $\alpha = \frac{1}{2} + \frac{(\omega+K)}{2W}$. The difference between the reaction-diffusion matrix of Eq. (27) and of Eq. (61) is a cleavage matrix operator whose only nonzero terms are defined at the cells 0 and 1,

$$\overleftrightarrow{V}_s = \frac{1}{W}\begin{pmatrix} 1 & -1 \\ -1 & 1 \end{pmatrix}. \tag{62}$$

The Green's function of the cleaved chain, $\overleftrightarrow{d}$, can be obtained by solving Dyson's equation. This equation treats the cleavage operator as a perturbation and expresses the Green's function of the cleaved system in terms of the Green's function $\overleftrightarrow{D}$ of the infinite chain. Dyson's equation is written as

$$\overleftrightarrow{d}(\overleftrightarrow{I} + \overleftrightarrow{V}\overleftrightarrow{D}) = \overleftrightarrow{D}. \tag{63}$$

In Eq. (63) we have dropped the symbol $\tilde{X}$ for the sake of simplifying the notation but we will keep in mind that the Green's functions are Laplace transforms. Writing Eq. (63) in component form gives

$$d_{n,n'} + d_{n,0}V_{0,0}D_{0,n'} + d_{n,0}V_{0,1}D_{1,n'} + d_{n,1}V_{1,0}D_{0,n'} + d_{n,1}V_{1,1}D_{1,n'} = D_{n,n'}. \tag{64}$$

Let us find the Green's function for the semi-infinite chain with $n, n' \geq 1$. In that case, $d_{n,0}=0$ since there is no diffusion between cell 0 and cells in the positive semi-infinite chain. Equation (64) simplifies to

$$d_{n,n'} + d_{n,1}V_{1,0}D_{0,n'} + d_{n,1}V_{1,1}D_{1,n'} = D_{n,n'}. \tag{65}$$

Equation (65) can be expressed at the cell $n'=1$,

$$d_{n,1} + d_{n,1}V_{1,0}D_{0,1} + d_{n,1}V_{1,1}D_{1,0} = D_{n,1}. \tag{66}$$

Inserting the expression for the Green's function of the infinite chain given by Eq. (28) as well as Eq. (62) into Eq. (66) results in

FIG. 4. Two semi-infinite chains of endothelial cells obtained by severing the gap junctions between cells 0 and 1.

$$d_{n,1} = \frac{-1}{W}\frac{\tau^n}{\tau - 1}. \tag{67}$$

Inserting Eq. (67) into Eq. (65) leads to the sought Green's function,

$$\tilde{d}_{n,n'} = \frac{-1}{W}\frac{\tau^{|n-n'|+1} + \tau^{n+n'}}{\tau^2 - 1}. \tag{68}$$

The inverse Laplace transform of Eq. (68) gives the Green's function of the semi-infinite chain $D^s_{n,n'}$, that is for $n, n' \in [1, \infty]$,

$$D^s_{n,n'}(t) = e^{-Kt}e^{-2Wt}[I_{|n-m|}(2Wt) + I_{n+n'-1}(2Wt)] \tag{69}$$

The short-time propagator for the nonlinear reaction dynamics is therefore written as

$$D^s_{n,n'}(\delta t) = e^{-[K_1+p(K_2-K_1)]\delta t}e^{-2W\delta t}[I_{|n-n'|}(2W\delta t) + I_{n+n'-1}(2W\delta t)]. \tag{70}$$

Propagator [Eq. (70)] corresponds to a zero-flux boundary condition at the end of the semi-infinite chain.

A variety of other Green's function can be obtained using the IRT. These include, for instance, a segment of cells with finite length, an infinite chain with finite side branch [15]. Without derivation, we also write below the Green's function for a semi-infinite chain with absorbing boundary conditions at the end of the semi-infinite chain [37],

$$D^A_{n,n'}(\delta t) = e^{-[K_1+p(K_2-K_1)]\delta t}e^{-2W\delta t}[I_{|n-n'|}(2W\delta t) - I_{n+n'}(2W\delta t)]. \tag{71}$$

We note that in Eq. (71), the Green's function vanishes at n=0, thus imposing the absorbing condition. From a biological point of view, this propagator may represent a semi-infinite chain with its end embedded into the extracellular matrix (ECM) that serves as diffusion sink. The ECM is the extracellular component of a tissue that performs several functions such as providing support to the cells.

Figure 5 illustrates the time evolution of a calcium front originating at cell 10 from the end of a semi-infinite chain, calculated with Eqs. (70) and (71). Again here, we have used

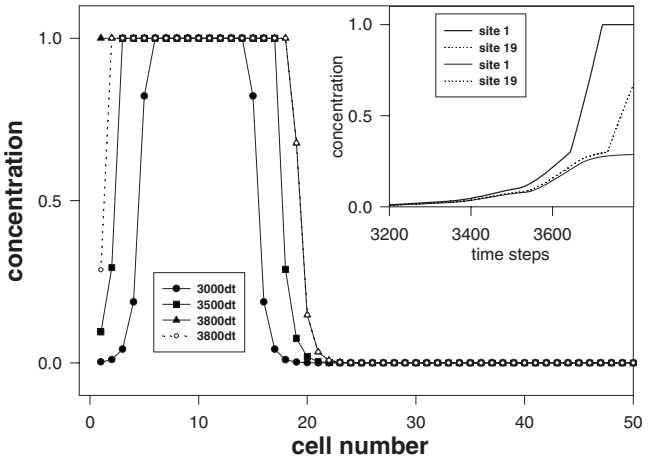

FIG. 5. Closed circles are for the semi-infinite system with zero-flux boundary conditions [propagator given by Eq. (70)] and the open are for the semi-infinite chain with the absorbing conditions at $n=0$ [propagator given by Eq. (71)]. The inset illustrates the time evolution of the concentration at the end site (site I) and its symmetrical counterpart with respect to the initial delta concentration (site 19). The thin solid line is for the absorbing conditions and the thick line for the semi-infinite chain with zero-flux conditions. The doted lines for the two types of boundary conditions overlap.

a short-time approximation for the modified Bessel function. The conditions of the calculations are: $W=0.7$, $K_1=-K_2=1$, $\delta t=0.01$, $u_c=0.3$. The initial condition corresponds to a delta concentration located at $n=10$ of magnitude $u(t=0)=0.55$.

With the zero-flux conditions, the concentration at the end cell (cell 1) remains at its maximum value of 1. The absorbing boundary conditions establish a concentration profile between cell 2 and 1. The propagator given by Eq. (71) reduces the concentration at cell 1 to a value significantly lower than 1 compatible with the large flux associated with the absorbing conditions at $n=0$. The calcium concentration of cell 1 (at the end of the semi-infinite chain) is therefore clearly dependent on the imposed boundary conditions. Away from the end of the semi-infinite chain, the calcium concentration front appears to be independent of the boundary conditions. The Green's function-based approach to solving the diffusion-reaction problem with nonlinear reaction dynamics is therefore providing a practical way to address problems with a variety of boundary conditions.

To investigate further the effect of the boundary conditions at the end of a semi-infinite chain of endothelial cells, we contrast the effect on composition of the propagator for the infinite chain of cells [Eq. (35)] and that with absorbing boundary conditions given by Eq. (71). For this we first consider an initial condition $u_m(t=0)=(u_c+\varepsilon)\delta_{m,1}$ where ε is some small positive number such that the embedding parameter at site $m=1$ takes the value 1. This may represent a fluctuation of calcium concentration just beyond the critical concentration. The composition at a subsequent time step, δt, at the site of cell 1, calculated with both propagators, will therefore be given by

$$u_1^I(\delta t) = e^{-K_2\delta t}e^{-2W\delta t}I_0(2W\delta t)(u_c+\varepsilon),$$

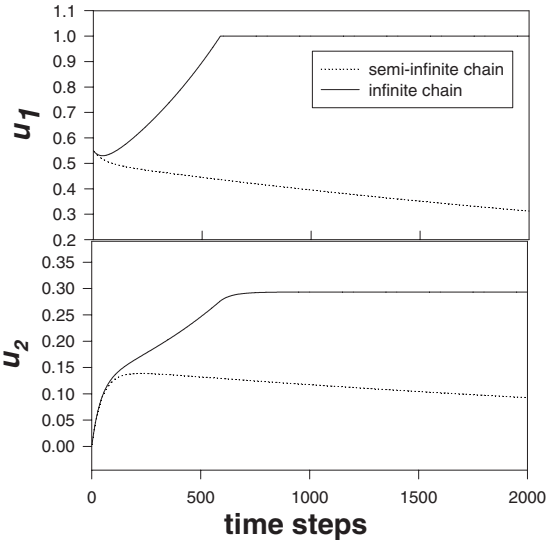

FIG. 6. Time evolution of the calcium concentration in cells 1 and 2 for an initial delta concentration located on cell 1. The initial concentration exceeds the threshold u_c.

$$u_1^A(\delta t) = e^{-K_2\delta t}e^{-2W\delta t}[I_0(2W\delta t) - I_2(2W\delta t)](u_c+\varepsilon). \tag{72}$$

In Eq. (72), the upper scripts I and A refer to the infinite chain and the semi-infinite one with absorbing boundary conditions. The effect of the absorbing boundary condition resides in the modified Bessel function, I_2 which reduces the rate of change of the calcium concentration at site 1 compared to that of the infinite chain. The difference between the two propagators will accumulate as one solves for the calcium concentration iteratively over numerous time steps. This is illustrated in Fig. 6 where we report the calcium concentration at sites 1 and 2 when we apply the initial condition $u_m(t=0)=0.55\delta_{m,1}$ to the infinite chains and the semi-infinite chain with absorbing boundary conditions. In this figure we have taken $W=0.6$, $K_1=-K_2=1$, $\delta t=0.01$, $u_c=0.3$. These conditions correspond to propagation failure. We have verified that one obtains similar results when the time step is reduced by a factor of two, indicating that the Green's function-based algorithm has converged. One sees clearly in the figure that the initial condition grows to a nonpropagating profile in the case of the infinite chain with the maximum centered on site 1. In contrast the calcium concentration at site 1 and 2 in the semi-infinite chain decays in spite of the initial concentration that exceeds the threshold, u_c.

This original example illustrates the importance of the architecture of the network of endothelial cells (e.g., infinite chain versus semi-infinite chain with absorbing boundary conditions) on the behavior of endothelial cells relative to their Ca^{2+} dynamics and concentration. Cell 1 is saturated in calcium in the infinite chain while it is depleted in the semi-infinite structure.

In summary, we have shown that the calcium dynamics of cells in the vicinity of the end of the semi-infinite chain is strongly dependent on the boundary conditions. We have demonstrated that the behavior of the semi-infinite chain

with absorbing boundary conditions, a simple model of a multicellular structure with an end in contact with the extracellular matrix, suggests behavioral differentiation between cells at the end and cells embedded within the chain.

IV. CONCLUSIONS

We have developed a Green's function-based (i.e., propagator-based) approach to solving nonlinear reaction-diffusion problems in networks of endothelial cells. The decoupling between the nonlinear reaction dynamics and the linear diffusion makes our approach compatible with the interface response theory (IRT) [16,38] which enables the calculation of the diffusion Green's function of nontrivial networks of cells. We demonstrated that our approach leads to the propagation of calcium wave fronts in a chain of endothelial cells with Ca^{2+} nonlinear reaction dynamics and transmembrane diffusion. More specifically, we showed that our model is in qualitative agreement with previously reported observations of transition between propagation and propagation failure as the strength of the diffusion constant is varied relative to the reaction constant. Our approach also enables the derivation of the propagator for a semi-infinite chain of cells with various boundary conditions. The primary result of this study consists of demonstrating that the Ca^{2+} dynamics of cells in the vicinity of the end of a semi-infinite chain with absorbing boundary conditions differs from that of cells deeply embedded in the chain. This behavior may be representative of multicellular structures imbedded in an extracellular matrix that serves as calcium diffusion sink. Although, we focused on calcium waves, the formalism and results presented in this paper would apply to other type of signals exhibiting a rather general nonlinear reaction dynamics with positive rate below a threshold and negative rate beyond that threshold. The findings predict that cells at the end of "dead-ended" branches of a cellular network would sense and/or respond differently to a variety of propagated signal wave. For instance, in branching morphogenesis [40], such as in the generation of the bronchial tree of the lung or the expansion of a vascular bed via angiogenesis, new branches arise from existing network elements (i.e., bronchus tube or blood vessel). In blood vessels, for example, a newly forming branch elongates behind a leading tip cell. In the mouse retina, initiation, and elongation of the neovessel is controlled by differential VEGF signaling along the length of the branch [41]. VEGF stimulates invasive behavior in the tip cell, but proliferation in stalk cell of the new branch. Additionally, a second molecular system initiated by the tip cell, the DLL4-Notch signaling axis [42], regulates stalk cell behavior such that new tip cells (and therefore new branches) are not aberrantly formed. While both of these signaling axes (VEGF and Notch) are externally applied and may not be recapitulated in the Green's function-based simulations, they highlight the different responses occurring in the cells of the forming branch. How these differences are established and what stimuli impart these differences are not clear. Perhaps, as implied by the theoretical work presented here, that network-wide signals, such as Ca^{2+} waves, alter the cellular milieu at the tip relative to elsewhere in the branch leading to responsive capability. Further experiments, guided by the predictions of the simulations, could provide important insight into the likely complex dynamics of these cellular structures.

ACKNOWLEDGMENT

This research was supported in part by the James S. McDonnell Foundation 21st Century Science Initiative in Studying Complex Systems.

[1] M. J. Bissell, A. Rizki, and I. S. Mian, Curr. Opin. Cell Biol. **15**, 753 (2003).
[2] R. K. Hansen and M. J. Bissell, Endocrine-Related Cancer **7**, 95 (2000).
[3] C. M. Nelson and M. J. Bissell, Annu. Rev. Cell Dev. Biol. **22**, 287 (2006).
[4] H. H. Q. Heng, BioEssays **29**, 783 (2007).
[5] M. H. Barcellos-Hoff, J. Mammary Gland Biology and Neoplasia **6**, 213 (2001).
[6] J. Kirshner, C. J. Chen, P. Liu, J. Huang, and J. E. Shively, Proc. Natl. Acad. Sci. U.S.A. **100**, 521 (2003).
[7] L. A. Davidson, Curr. Top. Dev. Biol. **81**, 113 (2008).
[8] A. G. Mikos, S. W. Herring, P. Ochareon, J. Elisseeff, H. H. Lu, R. Kandel, F. J. Schoen, M. Toner, D. Mooney, A. Atala, M. E. Van Dyke, D. Kaplan, and G. Vunjak-Novakovic, Tissue Eng. **12**, 3307 (2006).
[9] A. Ketchedjian, A. Linthurst Jone, P. Krueger, E. Robinson, K. Croutch, L. Wolfinbarger, and R. Hopkins, Ann. Thorac. Surg. **79**, 888 (2005).
[10] Q. K. Tran, K. Ohashi, and H. Watanabe, Cardiovasc. Res. **48**, 13 (2000).
[11] D. J. Watts and S. Strogatz, Nature (London) **393**, 440 (1998).
[12] H. G. Othmer and L. E. Scriven, J. Theor. Biol. **32**, 507 (1971); Ind. Eng. Chem. Fundam. **8**, 302 (1969).
[13] A. E. R. Turing, Philos. Trans. R. Soc. London, Ser. B **237**, 37 (1952).
[14] M. Eray, P. A. Deymier, J. H. Hoying, K. Runge, and J. O. Vasseur, Physica D **237**, 2777 (2008).
[15] P. A. Deymier, M. Eray, M. J. Deymier, K. Runge, J. B. Hoying, and J. O. Vasseur, Phys. Rev. E **81**, 041915 (2010).
[16] L. Dobrzynski and H. Puszkarski, J. Phys.: Condens. Matter **1**, 1239 (1989).
[17] P. De Koninck and H. Schulman, Science **279**, 227 (1998).
[18] E. Plahte, J. Math. Biol. **43**, 411 (2001).
[19] E. Plahte and L. Oyehaug, Physica D **226**, 117 (2007).
[20] A. Carpio and L. L. Bonilla, Phys. Rev. Lett. **86**, 6034 (2001).
[21] J. P. Keener, SIAM J. Appl. Math. **47**, 556 (1987).
[22] K. Kladko, I. Mitkov, and A. R. Bishop, Phys. Rev. Lett. **84**, 4505 (2000).
[23] J. W. Cahn, J. Mallet-Paret, and E. S. Van Vleck, SIAM J. Appl. Math. **59**, 455 (1998).
[24] J. Nakai, G. Salama, S. S. Segal, M. I. Kotlikoff, Y. N. Tallini,

J. F. Brekke, B. Shui, R. Doran, and Seong-min Hwang, Circ. Res. **101**, 1300 (2007).
[25] *"Computational Cell Biology," Interdisciplinary Applied Mathematics*, edited by C. P. Fall, E. S. Marland, J. M. Wagner, and J. J. Tyson (Springer, New York, 2000), Vol. 20.
[26] J. Sneyd and K. Tsaneva-Atanasova, in *Understanding calcium Dynamics: Experiments and Theory*, edited by M. Falcke and D. Malchow (Springer-Verlag, Berlin; Heidelberg, 2003).
[27] J. Keizer, G. D. Smith, S. Ponce-Dawson, and J. E. Pearson, Biophys. J. **75**, 595 (1998).
[28] S. Ponce Dawson, J. Keizer, and J. E. Pearson, Proc. Natl. Acad. Sci. U.S.A. **96**, 6060 (1999).
[29] H. Oktem, Nonlinear Anal. **63**, 336 (2005).
[30] H. M. Hardin and J. H. van Schuppen, Lect. Notes Control Inform. Sci. **341**, 431 (2006).
[31] J. G. Kirkwood, J. Chem. Phys. **3**, 300 (1935).
[32] R. Ravelo, J. Aguilar, M. Baskes, J. E. Angelo, B. Fultz, and B. L. Holian, Phys. Rev. B **57**, 862 (1998).
[33] J. H. He, Int. J. Mod. Phys. B **20**, 1141 (2006).
[34] F. Shakeri and M. Dehghan, Phys. Scr. **75**, 551 (2007).
[35] R. D. Mattuck, *A Guide to Feynman Diagrams in the Many-Body Problem* (McGraw-Hill, New York, 1992).
[36] P. Ramond, *Field Theory: A Modern Primer* (The Benjamin/Cummings Publishing Company, Inc, Melo Park, CA, 1981).
[37] P. A. Deymier, J. O. Vasseur, and L. Dobrzynski, Phys. Rev. B **55**, 205 (1997).
[38] L. Dobrzynski, Surf. Sci. Rep. **6**, 119 (1986).
[39] *Handbook of Mathematical functions*, edited by M. Abramowitz and I. A. Stegun, Eds. (Dover Publications, New York, 1972).
[40] M. Affolter, R. Zeller, and E. Caussinus, Nat. Rev. Mol. Cell Biol. **10**, 831 (2009).
[41] H. Gerhardt, M. Golding, M. Fruttiger, C. Ruhrberg, A. Lundkvist, A. Abramson, M. Jeltsch, C. Mitchell, K. Alitalo, and D. Shima, J. Cell Biol. **161**, 1163 (2003).
[42] M. Hellström, L. K. Phng, J. J. Hofmann, E. Wallgard, L. Coultas, P. Lindblom, J. Alva, A. K. Nilsson, L. Karlsson, and N. Gaiano, Nature (London) **445**, 776 (2007).